Available online at www.sciencedirect.com
ScienceDirect
Journal of Solid State Chemistry 179 (2006) 3763–3767
JOURNAL OF SOLID STATE CHEMISTRY
www.elsevier.com/locate/jssc

Crystal structure and magnetic properties of the coupled spin dimer compound $SrCu_2(TeO_3)_2Cl_2$

Rie Takagi[a], Mats Johnsson[a,*], Reinhard K. Kremer[b], Peter Lemmens[c]

[a]*Department of Inorganic Chemistry, Stockholm University, S-10691 Stockholm, Sweden*
[b]*Max Planck Institute for Solid State Research, Heisenbergstrasse 1, D-70569 Stuttgart, Germany*
[c]*Institute for Physics of Condensed Matter, TU Braunschweig, Mendelssohnstr. 3, D-38106 Braunschweig, Germany*

Received 5 June 2006; received in revised form 10 August 2006; accepted 13 August 2006
Available online 18 August 2006

Abstract

Single crystals of the strontium copper tellurium oxochloride $SrCu_2(TeO_3)_2Cl_2$ were synthesized via solid-gas reactions in sealed evacuated silica tubes. The compound crystallizes in the monoclinic system, space group $P2_1$, $a = 7.215(2)$, $b = 7.2759(15)$, $c = 8.239(2)$ Å, $\beta = 96.56(4)^\circ$, $Z = 2$. The building units are $[SrO_6Cl_2]$ irregular polyhedra, $[CuO_4]$ and $[CuO_3Cl]$ square planes, $[TeO_3E]$ tetrahedra and $[TeO_{3+1}E]$ trigonal bipyramids; E being the $5s^2$ lone pair of Te(IV). The Cu atoms can be regarded as forming a chain of weakly connected dimers. The magnetic susceptibility of the compound shows a broad maximum typical for antiferromagnetic spin fluctuations with a non-magnetic ground state. A Heisenberg spin model with coupled $s = 1/2$ dimers leads to a satisfactory fitting of the experimental data.

Keywords: Oxohalide; Lone pair elements; Crystal structure; Spin dimers; Antiferromagnetism

1. Introduction

Transition metal oxohalides containing elements such as Te^{4+} with stereochemically active lone pairs have proved to constitute a family of compounds showing a rich variability of low-dimensional arrangements of the transition metal ions. Both the lone-pair elements and the halides can act as "chemical scissors" reducing the dimensionality of the arrangement of the transition metal ions [1–2]. In this type of oxohalides the transition metals are normally more halophilic than Te^{4+} that is more "oxophilic". This difference in chemical affinities leads to tellurite building groups, e.g. pyramidal TeO_3^{2-} or see-saw TeO_{3+1}^{4-} groups, linking the transition metals that can coordinate both oxide- and halide ions. At the same time the one sided coordination of the tellurite groups and the fact that halide ions show a low coordination number of metals in this type of compounds helps to cut down the dimensionality of the arrangement of the metals in the structure.

The aim of the present study was to investigate how an alkaline earth metal such as Sr acts in this chemical environment. Sr^{2+} is known to accept bonds to both oxygen and halides and such a relatively big cation can accept a higher coordination than the other cations involved. The study yielded the new compound $SrCu_2(TeO_3)_2Cl_2$, it is isostructural with $BaCu_2(TeO_3)_2Cl_2$ [3], However, no physical properties have been reported for the latter compound. To our best knowledge the new compound is the first transition metal oxohalide compound containing all three of Sr^{2+}, Cu^{2+}, and Te^{4+}.

2. Experimental

The synthesis of $SrCu_2(TeO_3)_2Cl_2$ was made by chemical reactions in sealed evacuated silica tubes. SrO (ABCR, 99.95%), $CuCl_2$ (Avocado Research Chemicals, +98%), CuO (Avocado Research Chemicals, +99%), TeO_2 (ABCR, +99%) were used as starting materials. SrO:$CuCl_2$:CuO:TeO_2 were mixed in the stoichiometric molar

*Corresponding author. Fax: +46 8 15 21 87.
E-mail addresses: takagi@inorg.su.se (R. Takagi), matsj@inorg.su.se (M. Johnsson), rekre@fkf.mpg.de (R.K. Kremer), p.lemmens@tu-bs.de (P. Lemmens).

0022-4596/$ - see front matter © 2006 Elsevier Inc. All rights reserved.
doi:10.1016/j.jssc.2006.08.017

ratio 1:1:1:2 in a mortar and put into a silica tube (length ~5 cm) which was then evacuated. The tube was heated for 60 h at 920 K in a muffle furnace. The product appeared as bright green small single crystals. The crystals are non-hygroscopic.

Single-crystal X-ray data was collected on a STOE IPDS image-plate rotating anode diffractometer with use of graphite-monochromatized Mo $K\alpha$ radiation, $\lambda = 0.71073$ Å. The intensities of the reflections were integrated using the STOE software. Numerical absorption correction was performed with the programs X-red [4] and X-shape [5]. The structure was solved by direct methods (SHELXS97) [6] and refined by full matrix least squares on F^2 using the program (SHELXL) [7]. All atoms are refined with anisotropic temperature parameters. Molecular graphics were prepared with the program DIAMOND [8]. Experimental parameters, atomic coordinates and selected interatomic distances for $SrCu_2(TeO_3)_2Cl_2$ are reported in Tables 1, 2, and 3 respectively.

The sample used for the magnetic susceptibility measurement was characterized with powder X-ray diffraction (PXRD) data obtained with a Guiner–Hägg focusing camera with subtraction geometry. Cu$K\alpha_1$ radiation ($\lambda = 1.54060$ Å) where used and silicon, $a = 5.430880(35)$ Å, was added as internal standard. The recorded films were read in an automatic film scanner and the data were evaluated using the programs SCANPI [9] and PIRUM [10]. The magnetic susceptibility data were collected using a SQUID magnetometer (MPMS, Quantum Design) using a sample of $m = 2.995$ mg weight in a silica tube.

Table 1
Crystal data for $SrCu_2Te_2O_6Cl_2$

Empirical formula	$SrCu_2Te_2O_6Cl_2$
Formula weight	636.80
Temperature	291(2)
Wavelength	0.71073
Crystal system	Monoclinic
Space group	$P2_1$
Unit cell dimensions	$a = 7.215(2)$Å
	$b = 7.2759(15)$Å
	$c = 8.239(2)$Å
	$\beta = 96.56(4)^\circ$
Volume (Å^3)	429.7(2)
Z	2
Density (calculated)	4.922 g·cm^{-3}
Absorption coefficient	18.354 mm^{-1}
Absorption correction	Numerical
$F(0\,0\,0)$	564
Crystal colour	Green
Crystal habit	Rectangular box
Crystal size (mm)	$0.1 \times 0.05 \times 0.05$ mm^3
θ range for data collection	1.90°–28.15°
Index ranges	$-9 \leqslant h \leqslant 9$
	$-9 \leqslant k \leqslant 9$
	$-10 \leqslant l \leqslant 10$
Reflections collected	4147
Independent reflections	2011[R(int) = 0.0862]
Completeness to $\theta = 28.05^\circ$	99.3%
Refinement method	Full-matrix least squares on F^2
Data/restraints/parameters	2011/31/118
Goodness-of-fit on F^2	0.885
Final R indices [$I > 2\sigma(I)$]	$R_1 = 0.0445$
	w$R_2 = 0.0740$
R indices (all data)	$R_1 = 0.0831$
	w$R_2 = 0.0835$
Largest diff. peak and hole	1.60 and −1.70 (e Å^{-3})

Table 2
Atomic coordinates and equivalent isotropic displacement parameters for $SrCu_2(TeO_3)_2Cl_2$

Atom	x	y	z	U_{eq}[a] (Å^2)
Te(1)	0.36926(15)	0.90589(14)	0.11534(13)	0.0090(2)
Te(2)	0.14579(16)	0.17862(13)	0.73255(13)	0.0086(2)
Sr	0.3738(2)	0.5429(2)	0.43627(19)	0.0119(3)
Cu(1)	0.1386(3)	0.0401(3)	0.4118(2)	0.0117(4)
Cu(2)	0.8174(3)	1.0560(3)	0.0849(2)	0.0128(4)
Cl(1)	0.9447(6)	0.7766(6)	0.8733(6)	0.0163(9)
Cl(2)	0.3934(7)	0.7908(6)	0.7311(6)	0.0189(10)
O(1)	0.3022(15)	0.2081(14)	0.5580(13)	0.009(2)
O(2)	0.3086(16)	0.6536(16)	0.1156(14)	0.013(3)
O(3)	−0.0452(17)	0.0952(15)	0.5622(14)	0.015(3)
O(4)	0.3595(16)	0.9238(17)	0.3450(14)	0.016(3)
O(5)	0.0415(16)	0.4163(18)	0.7446(14)	0.017(3)
O(6)	0.3740(17)	0.3697(16)	0.8756(15)	0.018(3)

[a] U(eq) is defined as one-third of the trace of the orthogonalized U tensor.

3. Result and discussion

3.1. Crystal structure

The Te(1) atom has a pyramidal [Te(1)O_3] coordination. Taking the presence of the stereochemically active $5s^2$ lone pair of Te(1) (designated E) into account the coordination becomes a distorted tetrahedron [Te(1)O_3E]. The Te–O bond distances are in the range 1.864–1.906 Å. The Te(2) atom has a [Te(2)O_{3+1}] see-saw coordination. Including the stereochemically active lone pair the coordination becomes a distorted trigonal bipyramid [Te(2)O_{3+1}E] with the lone pair in the equatorial plane. Three of the Te–O bond distances are in the range 1.893–1.948 Å and the forth bond is at 2.364 Å.

The Cu(1) atom is coordinated by four O atoms forming a distorted [Cu(1)O_4] square plane with Cu–O bonds in the range 1.939–2.004 Å. A Cl(1) atom is located 2.919 Å away and complete a square pyramidal coordination [Cu(1)O_4Cl], however, this Cl-atom gives only a negligible contribution to the bond valence sum [11] giving for hand that it should not be considered as bonded. The Cu(2) atom is coordinated by three O atoms and one Cl(1) forming a distorted square plane [Cu(2)O_3Cl], the three Cu–O bond distances are in the range 1.928–1.988 Å and the Cu–Cl distance is 2.347 Å. A distorted [CuO_3Cl_3] octahedron is formed if also the two more far away laying Cl atoms are taken into account. However, those Cu–Cl

Table 3
Selected bond lengths (Å) and bond angles (°) for $SrCu_2(TeO_3)_2Cl_2$

Te(1)–O(6)^{i}	1.864(12)	Sr–O(4)	2.871(12)
Te(1)–O(2)	1.887(12)	Sr–Cl(2)^{iii}	2.935(5)
Te(1)–O(4)	1.906(11)	Sr–Cl(2)	3.016(5)
Te(2)–O(5)	1.893(13)	Cu(1)–O(5)^{iv}	1.944(12)
Te(2)–O(1)	1.939(11)	Cu(1)–O(4)^{v}	1.939(12)
Te(2)–O(3)	1.948(12)	Cu(1)–O(3)	1.957(12)
Te(2)–O(6)	2.364(12)	Cu(1)–O(1)	2.004(11)
Sr–O(3)^{ii}	2.403(13)	Cu(2)–O(5)^{i}	1.928(13)
Sr–O(4)^{iii}	2.628(11)	Cu(2)–O(2)^{vi}	1.928(12)
Sr–O(1)^{i}	2.624(11)	Cu(2)–O(6)^{i}	1.988(12)
Sr–O(1)	2.706(11)	Cu(2)–Cl(1)^{vii}	2.347(5)
Sr–O(2)	2.751(12)		
O(6)^{I}–Te(1)–O(2)	95.3(5)	O(4)^{iii}–Sr–Cl(2)^{iii}	72.7(3)
O(6)^{I}–Te(1)–O(4)	96.8(5)	O(1)^{I}–Sr–Cl(2)^{iii}	74.8(3)
O(2)–Te(1)–O(4)	91.8(5)	O(1)–Sr–Cl(2)^{iii}	75.8(2)
		O(2)–Sr–Cl(2)^{iii}	77.0(3)
O(5)–Te(2)–O(1)	101.9(5)	O(4)–Sr–Cl(2)^{iii}	119.0(3)
O(5)–Te(2)–O(3)	94.0(5)	O(3)^{ii}–Sr–Cl(2)	81.7(3)
O(1)–Te(2)–O(3)	85.6(5)	O(4)^{iii}–Sr–Cl(2)	71.4(3)
O(5)–Te(2)–O(6)	72.2(5)	O(1)^{i}–Sr–Cl(2)	75.6(3)
O(1)–Te(2)–O(6)	82.7(4)	O(1)–Sr–Cl(2)	103.5(2)
O(3)–Te(2)–O(6)	159.6(4)	O(2)–Sr–Cl(2)	125.9(3)
		O(4)–Sr–Cl(2)	68.3(2)
O(3)^{ii}–Sr–O(4)^{iii}	133.9(4)	Cl(2)^{iii}–Sr–Cl(2)	140.86(7)
O(3)^{ii}–Sr–O(1)^{i}	143.6(3)		
O(4)^{iii}–Sr–O(1)^{i}	63.8(3)	O(5)^{iv}–Cu(1)–O(4)^{v}	96.8(5)
O(3)^{ii}–Sr–O(1)	84.9(4)	O(5)^{iv}–Cu(1)–O(3)	93.7(5)
O(4)^{iii}–Sr–O(1)	66.7(3)	O(4)^{v}–Cu(1)–O(3)	155.2(5)
O(1)^{i}–Sr–O(1)	127.8(2)	O(5)^{iv}–Cu(1)–O(1)	170.0(5)
O(3)^{ii}–Sr–O(2)	84.1(4)	O(4)^{v}–Cu(1)–O(1)	89.4(5)
O(4)^{iii}–Sr–O(2)	141.9(4)	O(3)–Cu(1)–O(1)	83.7(5)
O(1)^{I}–Sr–O(2)	86.4(3)		
O(1)–Sr–O(2)	126.9(3)	O(5)^{i}–Cu(2)–O(2)^{vi}	167.6(5)
O(3)^{ii}–Sr–O(4)	80.9(4)	O(5)^{i}–Cu(2)–O(6)^{i}	80.8(5)
O(4)^{iii}–Sr–O(4)	120.0(3)	O(2)^{vi}–Cu(2)–O(6)^{i}	97.1(5)
O(1)^{I}–Sr–O(4)	64.4(3)	O(5)^{i}–Cu(2)–Cl(1)^{vii}	86.4(4)
O(1)–Sr–O(4)	164.5(3)	O(2)^{vi}–Cu(2)–Cl(1)^{vii}	98.0(4)
O(2)–Sr–O(4)	57.9(3)	O(6)^{i}–Cu(2)–Cl(1)^{vii}	162.3(4)
O(3)^{ii}–Sr–Cl(2)^{iii}	136.0(3)		

Symmetry transformations used to generate equivalent atoms: (i) $1-x$, $0.5+y$, $1-z$; (ii) $-x$, $0.5+y$, $1-z$; (iii) $1-x$, $-0.5+y$, $1-z$; (iv) $-x$, $-0.5+y$, $1-z$; (v) x, $-1+y$, z; (vi) $1-x$, $0.5+y$, $-z$; (vii) $2-x$, $0.5+y$, $1-z$; (viii) x, y, $-1+z$.

distances are long (2.838 and 2.895 Å, respectively) and bond-valence sum calculations suggest that they should not be considered as bonded.

The Sr atom is coordinated by six O atoms and two Cl atoms to form the highly irregular polyhedron $[SrO_6Cl_2]$. The Sr–O distances are in the range 2.624–2.871 Å except for the Sr–O(3) distance that is only 2.403 Å. The two Sr–Cl distances are 2.935 and 3.016 Å, respectively. The eight ion coordination is supported by bond valence sum calculations.

The Te(1)O_3E and Te(2)O_{3+1}E units are connected by sharing corners to form $[Te_2O_6E_2]$ groups. Those groups are linked by the $[Cu(1)O_4]$ and the $[Cu(2)O_3Cl]$ units. If the long Cu–Cl distances are taken into account the Cu polyhedra form dimer chains along the *b*-axis, see Fig. 1a, and a sketch with exchange paths with the apical chlorines omitted is shown in Fig. 1b.

Each $[SrO_6Cl_2]$ polyhedron is linked to two others by face sharing so that infinite chains of $[SrO_6Cl_2]$ polyhedra develop along the *b*-axis. In addition each $[SrO_6Cl_2]$ polyhedron share edges with one $[Cu(1)O_4]$ and one [Te(1)O_3E], further there is corner sharing with one $[Cu(2)O_3Cl]$, one [Te(1)O_3E], three [Te(2)O_{3+1}E], and three $[Cu(1)O_4]$. An overview of the structure is shown in Fig. 2. The stereochemically active Te-atom lone pairs are pointing towards the space in between the Cl atoms in the crystal structure.

The compound $SrCu_2(TeO_3)_2Cl_2$ is isostructural to $BaCu_2(TeO_3)_2Cl_2$ [3]. The latter compound was isolated from hydrothermal solvents at supercritical temperatures. The structural elements discussed above together with the low symmetry have important implications also for the electronic properties of the two compounds. Both compounds are insulators with a large gap of at least 2 eV and contain TeO-groups in a non-centrosymmetric surrounding. Based on theoretical modeling for other transition metal oxo-halides with low dimensional coordinations [12] we expect a large electronic polarisability and a potential for optical nonlinearity, such as second harmonic generation [13].

4. Magnetic properties

The powder sample used for magnetic susceptibility measurements was found to be phase pure from powder X-ray data and to have the unit cell parameters $a = 7.2164(5)$ Å, $b = 7.2848(5)$ Å, $c = 8.2474(5)$ Å, $\beta = 96.678(6)^{\circ}$. The magnetic susceptibility $\chi(T)$ given in Fig. 3 for a field of 1000 G has a broad maximum at $T_{max} = 125$ K with a height of $\chi(T_{max}) = 1.39 \times 10^{-3}$ emu/mol Cu Oe. For lower temperatures the susceptibility is dominated by an increase that is attributed to defects or impurities; this is represented in Fig. 3 by a Curie–Weiss dependence with an impurity content of $x_{imp.} = 1.33\%$, a Weiss temperature of $\theta_{CW} = +2.5$ K, and $g = 2.01$.

The crystallographic structure and Cu oxohalide coordination discussed so far suggest a 2D network of more or less weakly coupled $s = 1/2$ spin dimers as a possible magnetic exchange topology. In Fig. 1b we show such a mapping of the crystal structure on a distorted honeycomb lattice, however, with very anisotropic couplings. We approximate the hierarchy of interactions by three coupling constants: a strong Cu(1)–Cu(2) dimer, a weaker Cu(2) chain and the weakest interchain Cu(1) coupling, denoted by J_1–J_3. The strength of the coupling based on the proximity of superexchange partners in combination with taking into account the direct Cu–Cu ionic distances, the latter increase as 3.34, 4.47 and 4.79 Å, leading to the J's that form the dimers and chains, respectively.

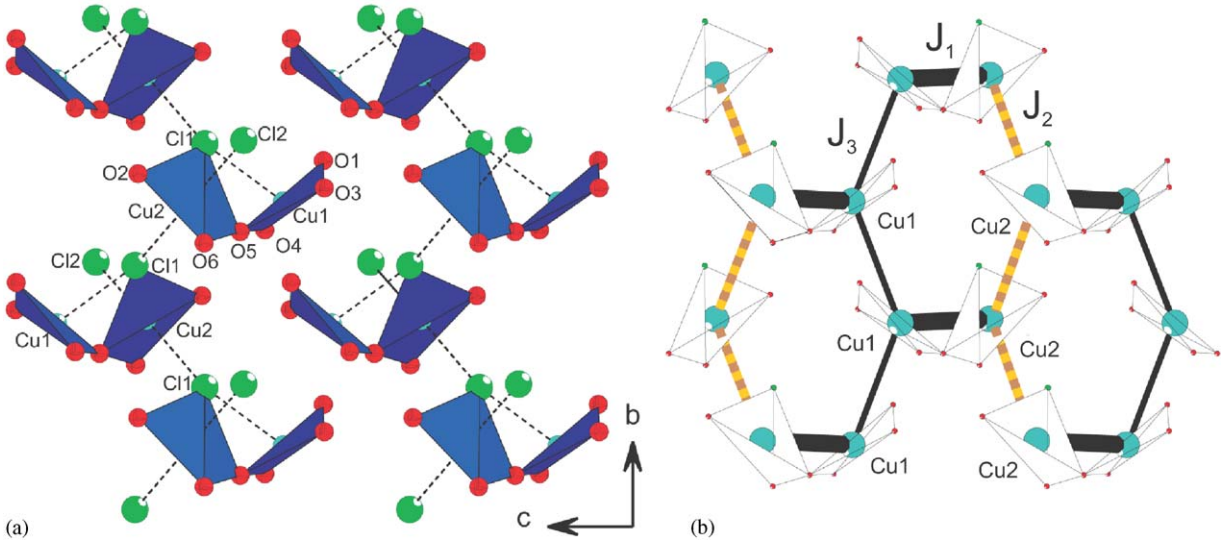

Fig. 1. (a) The $[Cu(1)O_4]$ and $[Cu(2)O_3Cl]$ units are connected by corner sharing. If the long Cu–Cl distances (dotted) are taken into account the $[Cu(1)O_4Cl]$ and the $[Cu(2)O_3Cl]$ polyhedra form chains of weakly connected dimers along [0 1 0]. (b) Mapping of the crystal structure on a strong J_1 Cu(1)–Cu(2) dimer, a weaker J_2 Cu(2) chain and an even weaker interchain J_3 Cu(1) coupling along the crystallographic b-axis, respectively.

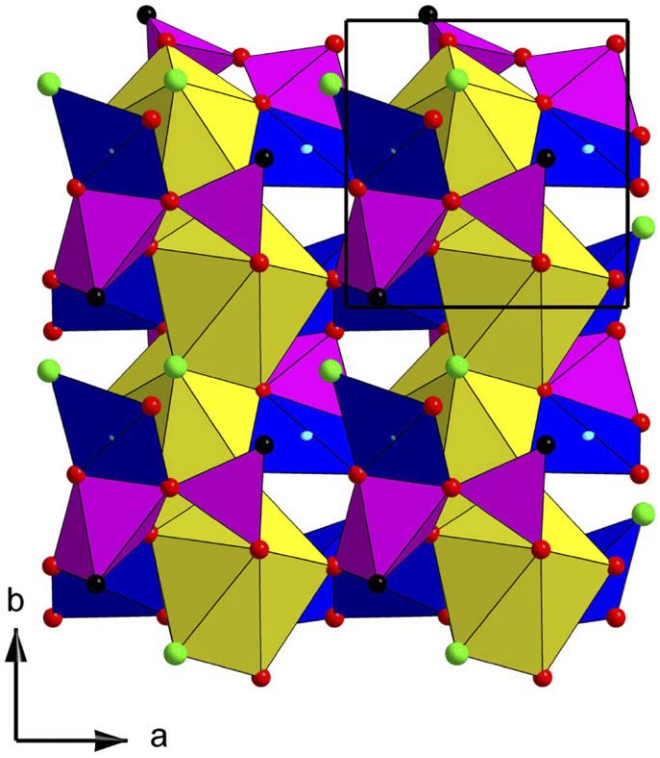

Fig. 2. Overview of the crystal structure for $SrCu_2(TeO_3)_2Cl_2$ along [0 0 1]. $[SrO_6Cl_2]$ (yellow), $[Cu(1)O_4]$ and $[Cu(2)O_3Cl]$ (blue), $[Te(1)O_3E]$ and $[Te(2)O_{3+1}E]$ (pink). Oxygen atoms are red, chlorine atoms are green, and the lone pairs on the Te atoms are represented by black spheres.

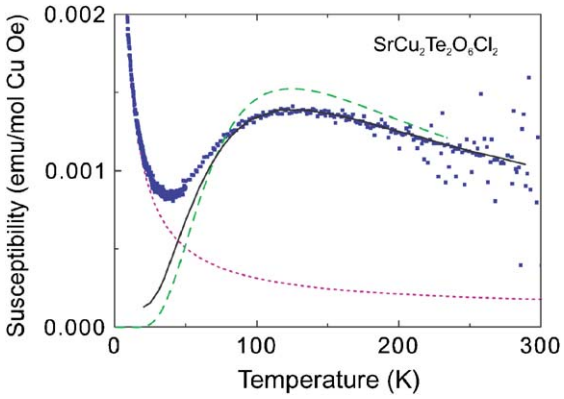

Fig. 3. Magnetic susceptibility of $SrCu_2(TeO_3)_2Cl_2$ in a field of 1000 G (symbols). The green dashed line corresponds to the Bleaney–Bowers equation for a spin dimer system with $J = -100$ K and the red dotted line represents the susceptibility of 1.33% paramagnetic impurities. The full line corresponds to a quantum Monte Carlo calculation for a system of coupled dimers with $J = 193$ K and an interdimer coupling of $J' = 77$ K. Data are compiled according to Johnston et al. [16].

Using the maximum position and the evolution of the susceptibility close to the maximum several simpler models can be tested that are used as a basis of the description. The decrease of the susceptibility observed for $T < T_{max}$ points to a non-magnetic ground state. Considering $s = 1/2$ states with an antiferromagnetic (AF) interaction, as realized in Cu^{2+}–$3d^9$ systems in oxygen or halide coordination, we start from spin arrangements that lead to a singlet ground state [14], i.e. AF spin dimers or coupled dimers that form spin ladders or chains.

The susceptibility of isolated AF dimers is described by the expression of Bleaney and Bowers [15]. A corresponding curve with a dimer exchange coupling of $J = 100$ K, $g = 2.01$ is shown in Fig. 3 as a dashed curve. The position of the maximum as well as the curvature of the susceptibility for temperatures $T > T_{max}$ are not in accordance simultaneously. As a next step we take a coupling of spin dimers via an interdimer coupling J' into account. For dimer ladders or chains the susceptibility $\chi(T)$ is modified

in the sense that the maximum in the susceptibility shifts to higher temperatures and is reduced in magnitude [16]. Unfortunately, due to the pronounced criticality of $s = 1/2$ there exist no analytic expressions of the susceptibility $\chi(T)$ for dimers coupled to ladders or chains. High temperature expansions or other approximations cannot be used for our purpose as their range of validity is limited to temperature regimes either larger or smaller than T_{max}. On the other hand, quantum Monte Carlo simulation data exists for a large range of coupling parameters J and J' of a ladder [14] or a chain [17] that can be compared to our experimental data to find an approximate description. We have scaled these results to our experimental data and found excellent agreement for the parameter set $J = 193\,K$ and $J' = 77\,\mathrm{K}$. The spin gap is of the same order of magnitude as J. Also the magnitude of the susceptibility is in good agreement with theory. The only free parameter in this scaling is an offset $\chi_0 = 1.1 \times 10^{-4}$ emu/mol Cu Oe that can be interpreted as a Van-Vleck contribution. Considering the exchange topology sketched in the inset of Fig. 3, we identify J by the Cu(1)–Cu(2) dimer coupling J_1 and J' by a combination of J_2 and J_3. The latter combination depends on details of the hybridizations and hopping matrix elements that go beyond the scope of this article. A microscopic description and identification of the exchange paths can be performed using ab initio band structure calculations following a down-folding of the effective Cu–Cu hoppings and tight binding analysis. Such a study has successfully be performed, e.g. for the lone pair oxohalide $Cu_2Te_2O_5Br_2$ that is interpreted as a weakly coupled Cu tetrahedron system [18].

5. Conclusion

We have identified the new oxohalide $SrCu_2(TeO_3)_2Cl_2$, and characterized its magnetic properties. The temperature dependence of the magnetic susceptibility points to a non-magnetic ground state and has been compared with a coupled spin dimer model. Additional two-dimensional couplings of the dimer are smaller compared to the dimer coupling and do not lead to long range antiferromagnetic coupling.

The new compound crystallize in the monoclinic system, space group $P2_1$. The compound is isostructural with the previously described compound $BaCu_2(TeO_3)_2Cl_2$ [3]. The synthesis of $SrCu_2(TeO_3)_2Cl_2$ was made by chemical reactions in sealed evacuated silica tubes from a stoichiometric starting mixture of $SrO{:}CuCl_2{:}CuO{:}TeO_2 = 1{:}1{:}1{:}2$.

There are two crystallographically different Cu-atoms; one showing a distorted $[CuO_4]$ square planar coordination, with an additional long distanced Cl atom outside the primary coordination sphere completing a square pyramidal $[CuO_4Cl]$ coordination. The other Cu atom has a distorted square planar $[CuO_3Cl]$ coordination and a distorted $[CuO_3Cl_3]$ octahedron is formed if also the two more far away laying Cl atoms are taken into account.

5.1. Supplementary materials

Supplementary material has been sent to Fachinformationzentrum Karlsruhe, Abt. PROKA, 76344 Eggenstein-Leopoldshafen, Germany (fax: +49 7247 808 666; e-mail: crysdata@fiz-karlsruhe.de), and can be obtained on quoting the deposit number CSD-416653.

Acknowledgment

This work has been carried out through financial support from the Swedish Research Council, the DFG priority programs SPP1073/1137, and the European Science Foundation, ESF-HFM.

References

[1] M. Johnsson, K.W. Törnroos, F. Mila, P. Millet, Chem. Mater. 12 (2000) 2853–2857.
[2] M. Johnsson, K.W. Törnroos, P. Lemmens, P. Millet, Chem. Mater. 15 (2003) 68–73.
[3] C.R. Feger, J.W. Kolis, Inorg. Chem. 37 (1998) 4046–4051.
[4] X-RED, Version 1.07, STOE & Cie GmbH, Darmstadt, Germany, 1996.
[5] X-SHAPE revision 1.09, STOE & Cie GmbH, Darmstadt, Germany, 1997.
[6] G.-M. Sheldrick, SHELXS-97—Program for the solution of Crystal Structures, Göttingen, 1997.
[7] G.-M. Sheldrick, SHELXL-97—Program for the refinement of Crystal Structures, Göttingen, 1997.
[8] K. Brandenburg, DIAMOND Release 2.1e, Crystal Impact GbR, Bonn, Germany, 2000.
[9] K.E. Johansson, T. Palm, P.E. Werner, J. Phys. Sci. Instrum. 13 (1980) 1289–1291.
[10] P.E. Werner, Arkiv för kemi 31 (1969) 513–516.
[11] I.D. Brown, D. Altermatt, Acta Cryst. B 41 (1985) 244–247.
[12] I.V. Kityk, M. Makowska-Janusik, M.D. Fontana, M. Aillerie, A. Fahmi, J. Appl. Phys. 90 (2001) 5542–5549.
[13] H.-L. Jiang, M.-L. Feng, J.-G. Mao, J. Sol. State Chem. 179 (2006) 1911–1917 (and references therein).
[14] P. Lemmens, G. Güntherodt, C. Gros, Phys. Rep. 375 (2003) 1–103.
[15] B. Bleaney, K.D. Bowers, Proc. Roy. Soc. Lond. A 214 (1952) 451–465.
[16] D.C. Johnston, M. Troyer, S. Miyahara, D. Lidsky, K. Ueda, M. Azuma, Z. Hiroi, M. Takano, M. Isobe, Y. Ueda, M.A. Korotin, V.I. Anisimov, A.V. Mahajan, L.L. Miller, cond-mat/0001147 (2000) 1–63.
[17] D.C. Johnston, R.K. Kremer, M. Troyer, X. Wang, A. Klümper, S.L. Bud'ko, A.F. Panchula, P.C. Canfield, Phys. Rev. B 61 (2000) 9558–9606.
[18] R. Valenti, T. Saha-Dasgupta, C. Gros, H. Rosner, Phys. Rev. B 67 (2003) 245110.